Energy Flow, Thrust, Charm and the Partonic Structure of the Pomeron

Christopher M. Cormack

H1 Collaboration

University of Liverpool, Oliver Lodge Laboratory, P.O. Box 147, Liverpool, L69 3BX, U.K.
email: cormack@hep.ph.liv.ac.uk

Abstract. Measurements are presented of the system X of the hadronic final state produced in deep–inelastic positron–proton diffractive scattering ($e^+p \to eXY$) using data collected in 1994 by the H1 experiment at HERA. Shown are the hadronic energy flow and charged particle spectra in the rest frame of the system X . Also presented is the average value of thrust ($\langle T \rangle$) as a function of $\frac{1}{M_X}$, where M_X is the invariant mass of the system X and the thrust p_T. The inclusive charm production cross section is also presented. The data are consistent with a picture in which the partonic structure of the diffractive exchange ($I\!P$) is dominated by gluons, and cannot be described if the $I\!P$ is composed primarily of quarks.

INTRODUCTION

The Deep–inelastic scattering cross section, of the form $ep \to eXY$ in which the hadronic final state is separated into two parts, X and Y, by a large gap in pseudo–rapidity have been measured to high precision by the H1 collaboration [1]. The system Y consists of a proton or other baryonic state of mass $M_Y < 1.6\,\mathrm{GeV}$. The system X is typically found to be of low mass, M_X, compared with the $\gamma^* p$ invariant mass W.

The rapidity gap events [1,2] have been found to be consistent with a diffractive production mechanism and the diffractive exchange, generically termed the pomeron ($I\!P$) has been interpreted as having a partonic structure that is dominated by gluons [3].

The picture of deep–inelastic diffraction described above has consequences for the nature of the hadronic final state. Quark and gluon dominated $I\!P$ exchanges lead to different final state topologies. A quark dominated $I\!P$ results in a two body parton configuration at lowest order, whereas a gluon dominated $I\!P$ will lead to a three body parton final state at leading order. In the $\gamma^* I\!P$ cms frame, quark dominated $I\!P$ exchange results in events in which the "struck

quark" and "remnant" are aligned along the $\gamma^* I\!P$ axis. Large contributions to the momentum transverse to this axis may arise from leading order QCD processes, such as QCD–Compton. However these are suppressed by a factor α_s.

If the pomeron is a gluon dominated object, more transverse energy is produced at leading order. This arises from the boson–gluon fusion process (BGF), in which the quark anti–quark pair from the hard subprocess are not necessarily aligned along the $\gamma^* I\!P$ axis; the quark propagator can have a finite virtuality, leading to the possibility of high p_T di–jet final states. For the gluon dominated pomeron the gluon exchanged in the t–channel enhances the wide angle soft gluon emissions [1]. For both the quark and gluon dominated $I\!P$ small contributions to the transverse momentum are generated by the intrinsic k_T of the partons, the hadronisation process and particle decays.

With a gluon dominated $I\!P$ more energy is deposited in the central region than is deposited with a quark dominated $I\!P$. This is investigated by studying the hadronic energy flow as a function of pseudo–rapidity, $\eta^* = -\ln\tan\frac{\theta^*}{2}$, where θ^* is the angle with respect to the direction of the exchanged boson, which defines the z axis. Similarly, the number of charged particles in the central region is higher in the gluon than in the quark dominated $I\!P$ picture. The partonic composition of the $I\!P$ is also investigated using thrust (T) [4] defined as:

$$T = \left(\frac{1}{\sum_{i=1}^{N}|\vec{p}_i|}\right) \cdot max \sum_{i=1}^{N} |\vec{p}_i \cdot \vec{a}| \qquad (1)$$

where $\vec{p}_i$ represents the momentum of particle i, in the rest frame of the system X and $\vec{a}$ is the unit vector along the thrust axis. Measurements are also made of the thrust p_T defined as:

$$p_T = \frac{1}{2}\sum_{i=1}^{N} |\vec{p}_i \cdot \vec{a}|\vec{a} \cdot \vec{n}_\perp \qquad (2)$$

where $\vec{n}_\perp$ is the unit vector perpendicular to the $\gamma^* I\!P$ axis.

For a quark dominated $I\!P$, the average value of thrust is expected to be larger and the thrust p_T smaller than for a gluon dominated $I\!P$

For the charged particle spectra comparisons are made with fixed target measurements of inclusive charged hadron production in deep–inelastic scattering, as a function of Feynman–x, ($x_F = \frac{2p_z^*}{M_X}$), where p_z^* is the component of the hadrons momentum in the z direction. Note that the relevant scale in diffractive DIS is the mass M_X of the system X. In non–diffractive DIS the appropriate scale is W, the mass of the complete hadronic final state. The comparisons are made with data for which $\langle M_X\rangle \approx \langle W\rangle$.

---

[1] This enhancement arises due to the gluon colour factor

A further sensitive discriminator between a quark and a gluon dominated $I\!P$ is the rate of charm production. This is expected to be high if the boson gluon fusion process is dominant and can only arise from the intrinsic charm content for a quark dominated $I\!P$.

For all measurements of the hadronic final state, comparisons are made with Monte Carlo predictions with different $I\!P$ parton distribution functions.

KINEMATICS AND EVENT SELECTION

The fraction of the initial proton's momentum carried by the $I\!P$, is given by $x_{I\!P} = \frac{q.I\!P}{q.p} \approx \frac{Q^2+M_X^2}{Q^2+W^2}$ where W is the invariant mass of the $\gamma^* p$ system, q^μ the 4–momentum of the virtual photon and p^μ that of the incident proton. The squared momentum transfer, $t = (P - Y)^2$ and the mass M_Y of the hadronic system Y are not measured. However the selection of the diffractive DIS sample described in [1,3] results in the restrictions $M_Y < 1.6\,\mathrm{GeV}$ and $|t| < 1\,\mathrm{GeV}^2$. The following kinematic range was selected for the energy flow and charged particle analysis: $7.5 < Q^2 < 100\,\mathrm{GeV}^2$, $0.05 < y < 0.6$, $x_{I\!P} < 0.025$ and $M_X > 3\,\mathrm{GeV}$. A complete description of the H1 detector can be found in [5].

For the energy flow measurement all clusters in the main calorimeters are boosted to the $\gamma^* I\!P$ centre–of–mass system. For the charged track spectra all primary vertex fitted tracks within $-1.31 < \eta < 1.31$ of the laboratory frame are taken and boosted to the $\gamma^* I\!P$ cms. For the thrust analysis a combination of tracks and clusters are used that improves the resolution in the thrust p_T measurement in the $\gamma^* I\!P$ cms. In the charm production analysis the decay $D^{*\pm} \to D^0 \pi^\pm_{slow} \to (K^\pm \pi^+)\pi^\pm_{slow}$ is used to reconstruct $D^{*\pm}$ mesons. The quantity $\Delta M = M_{D^{*\pm}} - M_{D^0}$ is used to determine the cross section measurement [2].

MONTE CARLO MODELS

Comparisons of theoretical expectations with measurements are made using the Monte Carlo generator RAPGAP2.02 [6]. This model, in conjunction with a detailed simulation of the H1 apparatus, was used to correct the distributions shown in the following for the acceptance and resolution of the H1 apparatus. RAPGAP treats diffractive interactions as inelastic $eI\!P$ collisions, the pomeron being considered to have partonic substructure. In addition to the $\mathcal{O}(\alpha)$ quark parton model diagram ($eq \to eq$), boson–gluon fusion ($eg \to eq\bar{q}$) and QCD–Compton ($eq \to eqg$) processes are generated according to the $\mathcal{O}(\alpha\alpha_s)$ matrix elements.

---

[2] The quantity ΔM is better resolved than the $D^{*\pm}$ mass itself.

Two sets of parton densities are used. In the first only quarks are permitted to contribute to the partonic structure of the pomeron at the starting scale for the DGLAP evolution $Q_0^2 = 2.5\,\mathrm{GeV}^2$. The second parameterisation features a "leading gluon" distribution at $Q^2 = Q_0^2$, in which gluons carry $\sim 80\%$ of the total momentum of the diffractive exchange. The latter set of parton densities was obtained from a fit to the diffractive structure function $F_2^{D(3)}$. The predictions of RAPGAP using these two sets of parton densities are hereinafter referred to as RG–Q and RG–QG, respectively.

RESULTS

Presented in figure 1a) is the energy flow $\frac{1}{N}\frac{dE}{d\eta^*}$ in the $\gamma^* I\!P$ cms for three different regions of M_X. Also shown are the predictions of the RG–Q and RG–QG simulations using the MEPS [7] and the CDM [8] fragmentation schemes. It can be seen that the Monte Carlo simulation with just quarks in the pomeron at the starting scale fails by a substantial amount to account for the observed energy flow in the central pseudo–rapidity region, $\eta^* \approx 0$. The data are well described by models in which the "leading gluon" parton distributions are used.

The charged track p_T^{*2} distribution is shown in figure 1b). The H1 data, at an average M_X of 10 GeV, are compared with EMC muon–proton DIS data at the slightly higher $\gamma^* p$ centre–of–mass energy of $< W >= 14\,\mathrm{GeV}$ [9]. The EMC data are at relatively high Bjorken–x (> 0.01), where the proton structure is dominated by quarks and are seen to lie significantly below the H1 data at large p_T. The RG–Q predictions are well below the H1 data. However the RG–QG expectations are in good agreement with the measured values.

The x_F distribution is shown in figure 1c). Again the data are compared with EMC results. Both the H1 and the EMC measurements give x_F distributions which fall with $|x_F|$. Whereas the EMC data are observed to be asymmetric about $x_F = 0$, the x_F distribution of the H1 data is approximately symmetric. This suggests that that in $\gamma^* I\!P$ interactions, the struck parton and the pomeron remnant are similar.

The mean charged track transverse momentum $\langle p_T^{*2} \rangle$ is shown as a function of x_F ("seagull plot") in figure 1d). The $\gamma^* I\!P$ data from H1 are again compared with $\gamma^* p$ data from the EMC and predictions from RAPGAP. It can be seen that the $\langle p_T^{*2} \rangle$ in the H1 data is significantly larger than observed by the EMC at all but the largest values of x_F, even though the average $\gamma^* I\!P$ centre–of–mass energy of the H1 data is slightly below the average $\gamma^* p$ centre–of–mass energy of the EMC data. This suggests that a large proportion of the H1 events involve a high $\hat{p}_T$ hard subprocess. The RG–Q (quark) fails to describe the level of $\langle p_T^{*2} \rangle$ in the struck quark or the remnant direction. Whereas the RG–QG models give a good description of the data.

The results of the thrust analysis are shown in figure 2a). Shown is the

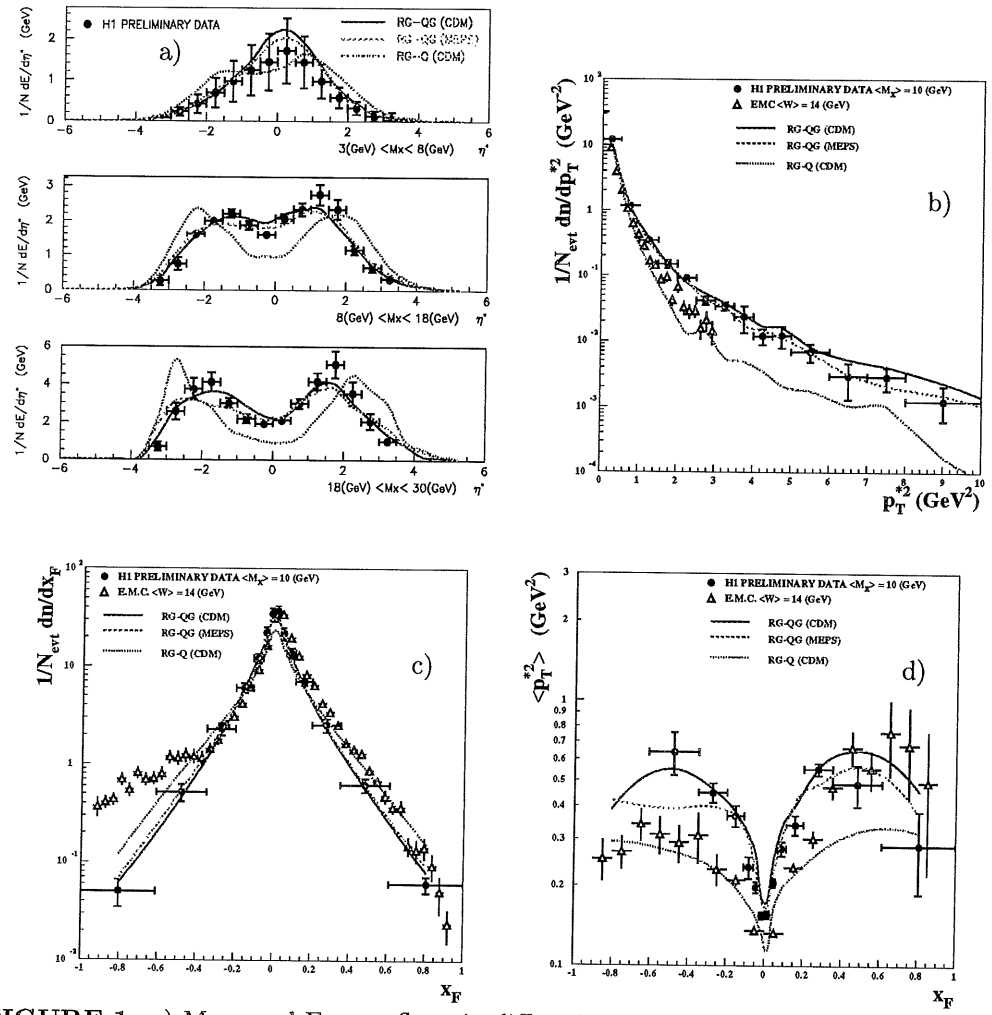

FIGURE 1. a) Measured Energy flows in diffractive DIS in the $\gamma^* I\!P$ frame as a function of M_X in the kinematic region $7.5 < Q^2 < 100\,\mathrm{GeV}^2$, $0.05 < y < 0.6$ and $x_{I\!P} < 0.025$. b) p_T^{*2} distribution showing H1 $\gamma^* I\!P$ data in the $\gamma^* I\!P$ frame together with EMC μp DIS data in the $\gamma^* p$ frame. c) the Feynman-x (x_F) distribution showing H1 $\gamma^* I\!P$ data in the $\gamma^* I\!P$ frame together with EMC μp DIS data in the $\gamma^* p$ frame. d) is the "Seagull" plot showing H1 $\gamma^* I\!P$ data in the $\gamma^* I\!P$ frame together with EMC μp DIS data in the $\gamma^* p$ frame. Each distribution is compared with the predictions of RAPGAP with various $I\!P$ parton distributions.

average value of thrust as a function of $1/M_X$ in 7 M_X intervals running from 4 to 36 GeV. The data show that the $\langle T \rangle$ increases with M_X. Given that the average particle multiplicity also increases, this implies that the final state is not isotropic, but exhibits a growing back to back correlation in the energy flow with increasing M_X. Also shown in figure 2a) are data from e^+e^- annihilation experiments [10] in which $M_X = \sqrt{s_{ee}}$, where s_{ee} is the centre–of–mass energy of the e^+e^- collision. The $1/M_X$ slopes are compatible, however the average thrust values are systematically lower for all M_X values in the diffractive data. This is consistent with the expectations of a "gluon dominated" exchange, in which higher order QCD radiation associated with the boson–gluon fusion process can occur.

Shown in figure 2b is the fraction of events with high thrust p_T^2 as a function of $\log(M_X)$. The data show that at high masses approximately 64% of events have a $p_T^2 > 1\,\mathrm{GeV}^2$ and approximately 38% have a $p_T^2 > 3\,\mathrm{GeV}^2$. This suggests that a significant number of events have a high p_T subprocess.

The charm cross section, is determined for the kinematic region $10 < Q^2 < 100\,\mathrm{GeV}^2$, $0.06 < y < 0.6$, $x_{I\!P} < 0.05$, $M_Y < 1.6\,\mathrm{GeV}$, $|\eta(D^{*\pm})| < 1.5$ and $p_T(D^{*\pm}) > 1.0\,\mathrm{GeV}$ (η and p_T in the H1 laboratory frame). The result is $\sigma(e^+p \to e^+D^{*\pm}X\,Y) = (380\,^{+150}_{-120}\,(stat)\,^{+140}_{-110}\,(syst))\,\mathrm{pb}$, obtained from a fit to the quantity ΔM shown in figure 3). The "leading gluon" model predicts a value for the cross section of $\sigma \sim 200\,\mathrm{pb}$ which is consistent with the measured cross section. The quark dominated pomeron model however predicts a cross section of less than 10 pb, which is inconsistent at the 2σ level with the measured cross section.

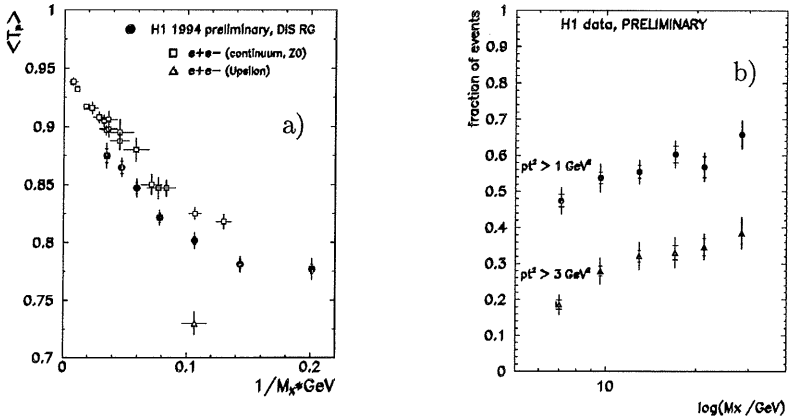

FIGURE 2. a) The average thrust as a function of $1/M_X$. Shown are the H1 diffractive data compared with e^+e^- annihilation data. b) The fraction of events with thrust $p_T^2 > 1\,(3)\,\mathrm{GeV}^2$. $F_2^{D(3)}$

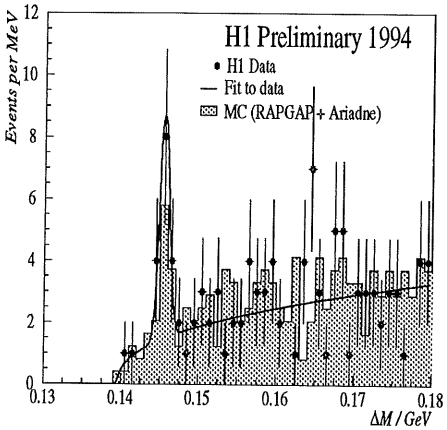

FIGURE 3. Distribution of the mass difference $\Delta M = M(K^-\pi^+\pi^\pm_{slow}) - M(K^-\pi^+)$, with a fitted curve of the form $a(\Delta M - M_{\pi^+})^b + Gaussian$ and a prediction from RAPGAP with the pomeron structure extracted from $F_2^{D(3)}$.

CONCLUSION

The high level of energy observed in the central region ($\eta^* \approx 0$) in the $\gamma^* I\!P$ centre–of–mass, the high p_T^{*2} tail and the high level of $\langle p_T^{*2} \rangle$ can only be explained in partonic models of diffractive scattering if the momentum of the pomeron is carried largely by gluons. This picture is confirmed by the thrust data and charm cross section. All hadronic final state analyses are consistent with the "leading gluon" parameterisation and cannot be explained by a quark dominated $I\!P$.

REFERENCES

1. H1 Collaboration, Phys. Lett. **B348** (1995) 681.
2. ZEUS Collaboration, Phys. Lett. **B315** (1993) 481.
3. H1 Collab., contributed paper, pa02–061, ICHEP July 1996, Warsaw, Poland. M. Dirkmann, these proceedings.
4. E. Farhi, Phys. Rev. Lett. **39** (1977) 1587.
5. H1 Collaboration, Nucl. Instr. Meth. **A368** (1997) 310.
6. H. Jung, Comp. Phys. Comm. **86** (1995) 147.
7. Yu. L. Dokshitzer, Phys. Rep. **58** (1980) 269.
8. L. Lönnblad, Comp. Phys. Comm. **71** (1992) 15.
9. EMC collaboration, Z. Phys. **C35** (1987) 417.
10. PLUTO collaboration, Z. Phys. **C12** (1982) 297.